International Journal of Rail Transportation

ISSN: (Print) (Online) Journal homepage: https://www.tandfonline.com/loi/tjrt20

Suspension parameters optimum of high-speed train bogie for hunting stability robustness

Yuan Yao , Guang Li , Guosong Wu , Zhenxian Zhang & Jiayin Tang

To cite this article: Yuan Yao , Guang Li , Guosong Wu , Zhenxian Zhang & Jiayin Tang (2020) Suspension parameters optimum of high-speed train bogie for hunting stability robustness, International Journal of Rail Transportation, 8:3, 195-214, DOI: 10.1080/23248378.2019.1625824

To link to this article: https://doi.org/10.1080/23248378.2019.1625824

INTERNATIONAL JOURNAL OF RAIL TRANSPORTATION
2020, VOL. 8, NO. 3, 195–214
https://doi.org/10.1080/23248378.2019.1625824

Suspension parameters optimum of high-speed train bogie for hunting stability robustness

Yuan Yao[a], Guang Li[a], Guosong Wu[a], Zhenxian Zhang[b] and Jiayin Tang[c]

[a]State Key Laboratory of Traction Power, Southwest JiaoTong University, Chengdu, China; [b]CRRC Qingdao Sifang Co., Ltd. Technology Center, Qingdao, China; [c]School of Mathematics, Southwest JiaoTong University, Chengdu, China

ABSTRACT

Hunting stability of high-speed train is an important objective for the optimization of bogie suspension parameters. An adequate hunting stability margin is required for the high-speed train. Besides, a remarkable ability to resist the influence caused by the disturbance of bogie suspension parameters and wheel-rail contact parameters on hunting stability is also required. In this paper, the concept of robustness of hunting stability is proposed, and the indexes for vehicle speed robustness, suspension parameter robustness, and wheel-rail contact equivalent conicity robustness are defined and chosen as the optimization objectives for the bogie suspension parameters. The multi-objective optimization method is used, which can optimize the key suspension parameters simultaneously to balance the multiple complicated and conflicting performance indexes, and six groups of typical suspension parameters are obtained by cluster analysis of Pareto frontier. The correlation between suspension parameters and each index is analysed by multivariate statistical analysis, and the optimization and matching rules for key suspension parameters of the high-speed train bogie based on hunting stability robustness are obtained. With the application of this method during the design process of suspension parameters, the hunting stability of high-speed trains in service can be greatly improved.

ARTICLE HISTORY
Received 11 March 2019
Revised 19 May 2019
Accepted 28 May 2019

KEYWORDS
High-speed train; hunting stability robustness; bogie; suspension parameters matching; multi-objective optimization

1. Introduction

With the increasing running speeds of the high-speed train, the lateral stability of the vehicle has received extensive attention. Although the lateral stability of the railway vehicles can be strengthened with the help of advanced mechanisms and active suspension systems [1–8], the optimization of the conventional passive suspension elements still could be considered as one of the efficient methods. Several studies on improving hunting stability of railway vehicles have been carried out [9–14]. The influences of suspension parameters on vehicle stability and curve passing performance are also taken into account in the optimization of bogie suspension parameters based on the vehicle hunting stability. The vehicle curve passing performance is often affected by the stiffness of secondary horizontal

CONTACT Yuan Yao yyuan8848@163.com State Key Laboratory of Traction Power, Southwest JiaoTong University, Chengdu, China

suspension, while the vehicle stability can be affected by more suspension parameters. In this paper, suspension parameters affecting the vehicle lateral dynamic performance are decoupled, and the optimization for the bogie horizontal suspension stiffness is conducted, except for the secondary horizontal stiffness. Reasonable matching for the bogie suspension parameters is conducive to improving the hunting stability margin and enhancing the ability to resist the influence caused by the disturbance of bogie suspension parameters and wheel-rail contact parameters on vehicle hunting stability. That is to say, the vehicles have strong adaptability for variation of suspension parameters and some track parameters. In this paper, the optimization of multi-parameters affecting the hunting stability of bogies is carried out for this multi-objective problem.

In general, the design optimization of a mechanical system is multidisciplinary, and the task is to find effective trade-off solutions for the complicated and conflicting design criteria [15,16]. In the suspension design of railway vehicles, the task is to search for a compromised design while considering lateral stability, curving performance, and ride quality. The genetic algorithm is known as one of the most powerful tools in global optimization and is particularly useful in design optimization problems of sophisticated nonlinear systems. He and McPhee [17] proposed the methodology via genetic algorithm, which can handle the conflicting requirements of rail vehicle design effectively. They also utilized the genetic algorithm to settle the curving performance optimization problem of a railway vehicle model with 21 DOF (Degree of Fredom). Johnsson [18] et al. optimized passive damping elements of bogie suspension by using the genetic algorithm, and optimized passive damping elements in the bogie suspensions can improve the safety and comfort of the railway vehicle. Seyed [19] et al. solved the wear/comfort Pareto optimization problem of bogie suspension by using the GA (Genetic Algorithm). A 50 degrees of freedom railway vehicle model developed has been studied, whose aim is to reduce wheel/rail contact wear and improve passenger ride comfort, and the Pareto-optimized values of the design parameters achieved here guarantee wear reduction and comfort improvement for railway vehicles. Uncertainties in the design parameters of the suspension system can negatively influence the dynamics behaviour of railway vehicles. Seyed [20] analysed the robustness of bogie suspension parameters achieved from the wear/comfort Pareto optimization problem. At present, most literature focus on the trade-off between vehicle running performance on tangent track, curve performance and vehicle wear performance for the suspension parameters optimization of railway vehicles.

The optimization and matching of bogie suspension parameters is particularly important for the design of vehicle hunting stability robustness. Therefore, the design for hunting stability of bogie suspension parameters is also a process of multi-objective optimization, and the hunting stability margin of vehicles, as well as the robustness of bogie suspension parameters and the track adaptability should be taken into account. In this regard, the robust hunting stability Pareto optimization of bogie suspension parameters is considered. A method for the optimization of key bogie suspension parameters based on vehicle hunting stability is presented in this paper. The design objectives for vehicle hunting stability are defined, and the multi-objective optimization method is adopted to optimize the key suspension parameters affecting the vehicle hunting stability simultaneously to find out the matching rules for bogie suspension parameters, which propose a method for the optimization and design of vehicle suspension parameters.

2. Hunting stability robustness

2.1. The vehicle linear dynamics model

In order to investigate the vehicle hunting stability, a simplified vehicle lateral dynamic model is established, as shown in Figure 1. The model is composed of seven rigid bodies, which are one carbody, two frames, and four wheelsets. The carbody and the frame have lateral, yaw and roll degrees of freedom, and the wheelsets have lateral and yaw degrees of freedom. The primary suspension is between the wheelset and the frame, which is composed of lateral, longitudinal and vertical positioning stiffness. Besides, the primary rotating arm axle box structure is considered in the model. The secondary suspension is between the carbody and the frame, which is composed of lateral, longitudinal and vertical stiffness, damping and anti-roll stiffness. In order to analyse the effects of series stiffness of the oil damper on vehicle stability, the yaw damper and the secondary lateral damper are established based on the Maxwell model that consists of spring and damper in series [21]. The dynamics model has 25 degrees of freedom. The linear stability of the established vehicle model is emphatically analysed in this paper; thus, the wheel-rail contact geometry is expressed by equivalent conicity, and the wheel-rail tangential force is calculated by linear Kalker theory. Referring to one type of high-speed EMU in China [22,23], the specific parameters of the model are shown in Appendix Table A1. The equation of the system dynamics model is as follows:

$$\mathrm{M}\ddot{\mathrm{x}}(\mathrm{t}) + \mathrm{C}\dot{\mathrm{x}}(\mathrm{t}) + \mathrm{K}\mathrm{x}(\mathrm{t}) = \mathrm{Q} \tag{1}$$

The **x** is the degree of freedom vector of the system. The matrices M, C, K, and Q are the mass, damping, stiffness and external force components of the system, respectively. For the motion equation of a single wheelset with an elastic primary suspension, the lateral and yaw movement of wheelset are coupled by the wheel-rail tangential forces [24,25]. The K is an asymmetric stiffness matrix, and the non-diagonal items represent

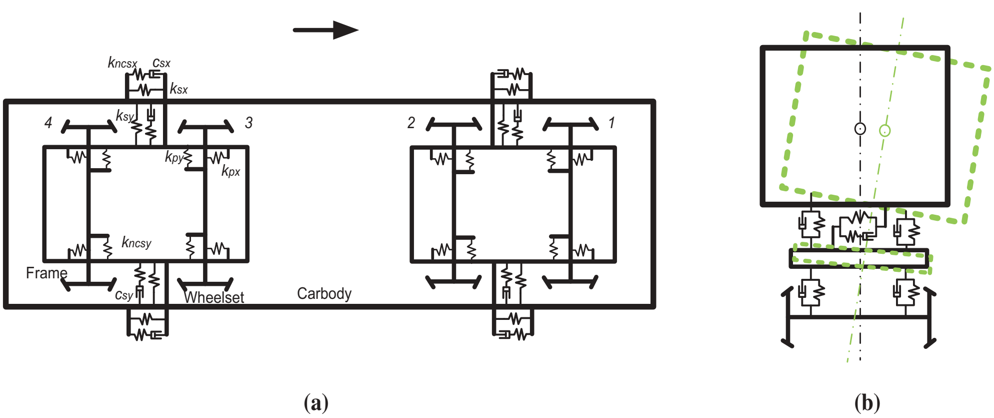

Figure 1. Simplified vehicle lateral dynamic model.

the coupling of the wheelset's lateral and yaw movement caused by the interaction of wheel and rail in tangential. The system damping C is related to the running speed v. In a period of hunting motion, if the input and the consumed energy are equal, the linear system is in the critical stability state. The corresponding speed v is the linear critical speed.

Due to the unsymmetrical nature of the stiffness matrix K, Equation (1) cannot be transformed into an uncoupled set of differential equations by means of conventional methods of modal analysis, i.e. using only real modes. A solution can still be effected though, by using the complex modal transformation [2,17]. To do this, Equation (1) is recast into the following state-space form,

$$\dot{\mathrm{y}}(\mathrm{t}) = \mathrm{Ay}(\mathrm{t}) \tag{2}$$

The vector $\mathbf{y}$ is the system state variable vector, and the system matrix A is given by,

$$\mathrm{A} = \begin{bmatrix} 0_{25\times25} & \mathrm{I}_{25\times25} \\ -\mathrm{M}^{-1}\mathrm{K} & -\mathrm{M}^{-1}\mathrm{C} \end{bmatrix} \tag{3}$$

The modal shapes and linear stability of the vehicle system are obtained by analysing the eigenvectors and eigenvalues of A.

It is necessary to take account of the vehicle running performance on tangent track and the curve passing performance when designing the bogie suspension parameters. According to the experience, the horizontal stiffness of the bogie secondary suspension has great influences on vehicle ride stability and curve passing performance, but has little effect on vehicle hunting stability. Moreover, the stiffness of the secondary air spring for the high-speed train varies in a small range. We mainly focus on the vehicle hunting stability in this paper; thus, the lateral stiffness of secondary suspension is not optimized. This paper mainly focuses on the key suspension parameters of bogie which affect the hunting stability of vehicles, such as the primary longitudinal stiffness *kpx*, the primary lateral stiffness *kpy*, the damping of yaw damper *csx*, the damping of secondary lateral damper *csy*, the yaw damper series stiffness *kncsx* and the secondary lateral damper series stiffness *kncsy*, which are chosen as optimization objects to improve the robustness of hunting stability for railway vehicles.

2.2. Stability robustness index

Horizontal suspension parameters of high-speed train bogies have a remarkable influence on the vehicle lateral dynamic performance, which mainly reflected in the lateral comfort, curve passing performance and hunting stability. Due to the high running speed, the vehicle hunting stability is the most important index, which must be got much attention in the design.

Errors that inevitably occur in the design and manufacture of bogie suspension components, and the creep or failure of rubber joints and hydraulic dampers, can result in the change of suspension stiffness and damping, and then affect the vehicle dynamics performances. In addition, the change of wheel-rail contact geometry caused by the rail deformation and the tread and rail head wear will also affect the vehicle dynamic performance. Therefore, a large hunting stability margin in a wide speed range is required for the high-speed train, as well as remarkable ability to resist the influence caused by the disturbance of bogie suspension parameters and wheel-rail contact parameters on vehicle lateral stability is required. That is to say, the trains need a strong adaptability for suspension parameters and wheel–rail interaction.

The vehicle speed robustness, suspension parameter robustness and wheel-rail equivalent conicity robustness defined as the robustness of hunting stability are taken into account in the optimization and matching for bogie suspension parameters. The eigenvalues of the system matrix are calculated for the vehicle linear dynamic model. The ratio of the real part of eigenvalues to the modulus corresponding to hunting mode regarded as the natural modal damping is defined as the linear stability index of the system, which is represented by ζ. When ζ is negative, it shows that the linear model is stable. The ζ_{200}, ζ_{350} and ζ_{500} are the stability indexes corresponding to the three speed conditions of 200, 350 and 500 km/h, and the corresponding equivalent conicity in this study are 0.05, 0.17 and 0.30, respectively. The smaller the index value, the more stable the system. In order to evaluate the influence of disturbance resulting from bogie suspension parameters and wheel-rail contact parameters on the hunting stability of vehicle, the suspension parameters are distributed in a certain range, and the stability indexes of the system are calculated with the different combined suspension parameters, and its standard deviation is defined as suspension parameters the robustness index. Similarly, the standard deviation of the stability index corresponding to the equivalent conicity distributed in a certain range of the system is defined as the equivalent conicity robustness index, denoted by $std(\zeta_{par})$ and $std(\zeta_{\zeta})$, respectively. The smaller the two index values, the smaller the influence of suspension parameters and equivalent conicity on the system stability, and the stronger the corresponding robustness. The suspension parameters robustness index is obtained by calculating the 1000 groups of suspension parameters with uniform distribution in the range of (±20%) and randomly combined, and the equivalent conicity robustness index is obtained by analysing the different equivalent conicity uniformly distributed in the range of 0.05–0.3 in this paper. The stability robustness index and corresponding calculation condition are shown in Table 1.

2.3. Multi-objective optimal

There is a significant difference between multi-objective optimization and single-objective optimization. The best solution which is usually regarded as the global maximum or minimum and known as the global optimal solution can be found in single-objective optimization. While it is difficult to find a solution to make all objective functions optimal because of the conflicts and incomparability between objectives for multi-objective optimization. That is to say, one solution may be the best for one

Table 1. Stability robustness index.

Index	Calculation condition		Description
	v (km/h)	ζ	
ζ_{200}	200	0.05	Linear stability index of 200 km/h
ζ_{350}	350	0.17	Linear stability index of 350 km/h
ζ_{500}	500	0.30	Linear stability index of 500 km/h
$std(\zeta_{par})$	350	0.17	Suspension parameter robustness index
$std(\zeta_{\zeta})$	350	0.17	Equivalent conicity robustness index

objective function, but not the best or even the worst for other objective functions. Therefore, there is usually a set of solutions, which cannot be compared for multi-objective optimization. These solutions are called nondominated solutions or Pareto optimal solutions. By having different design options, the decision-maker can choose any point from the solution set that meets the performance requirements.

Six suspension parameters, including the primary longitudinal stiffness *kpx*, the primary lateral stiffness *kpy*, the damping of yaw damper *csx*, the damping of secondary lateral damper *csy*, the yaw damper series stiffness *kncsx* and the secondary lateral damper series stiffness *kncsy* are optimized in this paper. Five optimization objectives, including the ζ_{200}, ζ_{350}, ζ_{500}, $std(\zeta_{par})$ and $std\ (\zeta_{\zeta})$ are considered. The multi-objective optimal design problem is stated as

$$\min\left\{\zeta_{200},\zeta_{350},\zeta_{500},std\left(\zeta_{par}\right),std\left(\zeta_{\zeta}\right)\right\} \tag{4}$$

The NSGA-II algorithm can keep the population diversity and improve the computational efficiency; thus, it is an effective algorithm for solving multi-objective problems. Therefore, a fast non-dominated sorting genetic algorithm NSGA-II with elitist strategy is selected for multi-objective optimization design in this study [26]. Most of the default settings of this algorithm are kept and only two parameters are changed. They are population size and generation number. In this study, the population size is set to 5000, and the number of generation is set to 100.

3. The multi-objective optimal results

The genetic algorithm NSGA-II was used in the multi-objective optimization for the above six groups of key bogie suspension parameters. The Pareto frontier and Pareto set for the parameters are obtained by iteration and updating suspension parameters to optimize the vehicle system performance toward the defined objectives, which are shown in Figure 2. The three coordinate axes represent the vehicle stability index ζ_{200}, ζ_{350}, and ζ_{500} corresponding to the speed of 200, 350, and 500 km/h, respectively. The smaller the value, the better the system stability is. The colour in the figure indicates the suspension parameter robustness index $std(\zeta_{par})$. The darker the color, the better the suspension parameter robustness is. That is, the suspension parameter changing within a certain range has a small influence on the vehicle hunting stability is small. The size of the point in the figure represents the equivalent conicity robustness index $std(\zeta_{\zeta})$. The larger the point size, the better the equivalent conicity robustness, which means that the wheel-rail contact geometry has little effect on vehicle stability, indicating a long vehicle tread turning period and a strong track adaptability.

The Pareto frontier illustrates the contradiction between optimization objectives. The system stability can be improved at the expense of the suspension parameters robustness, and the system stability is not completely negatively correlated with the equivalent conicity robustness for different speeds. Therefore, it is necessary to select the suitable objective values from the Pareto frontier that satisfies the design requirements, and then to acquire the corresponding suspension parameters.

Considering that it is difficult to deal with large amounts of data of Pareto frontier in Figure 2, the *K-Means* clustering method [27] is adopted in this study. After

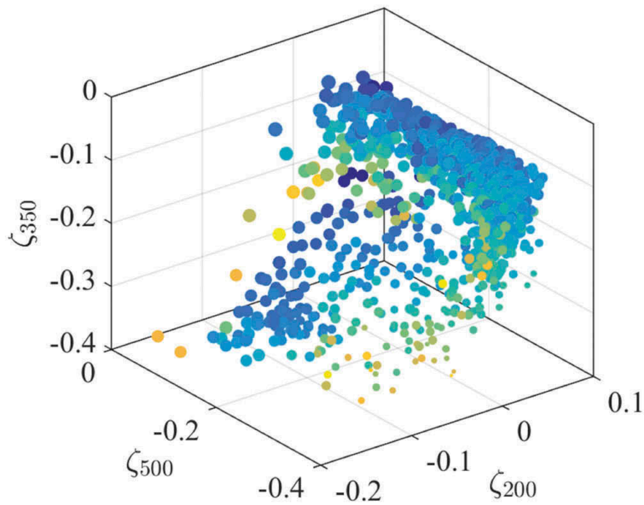

Figure 2. Pareto frontier of multi-objective optimization.

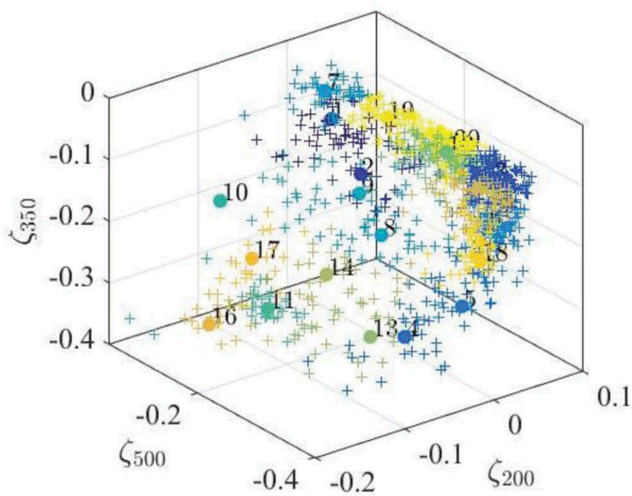

Figure 3. Cluster analysis of pareto frontier.

normalizing the Pareto frontier data, and clustering according to the spatial distance, the cluster centres are evenly distributed in the Pareto frontier. Twenty cluster centres are obtained by clustering the Pareto frontier, as shown in Figure 3. The clustering results of the suspension parameter robustness index $std(\zeta_{par})$ and the equivalent conicity robustness index $std(\zeta_{\zeta})$ are shown in Figure 4.

The 6 representative clusters were extracted from the 20 clusters for further analysis. Figure 5 is a radar chart corresponding to the five optimization objectives of the six cluster centres. The farther the coordinate axis in the radar chart is, the smaller the objective value is, which means a better objective performance. The objective values of ζ_{200} and ζ_{350} corresponding to 16th cluster are the smallest. The objective values of ζ_{500},

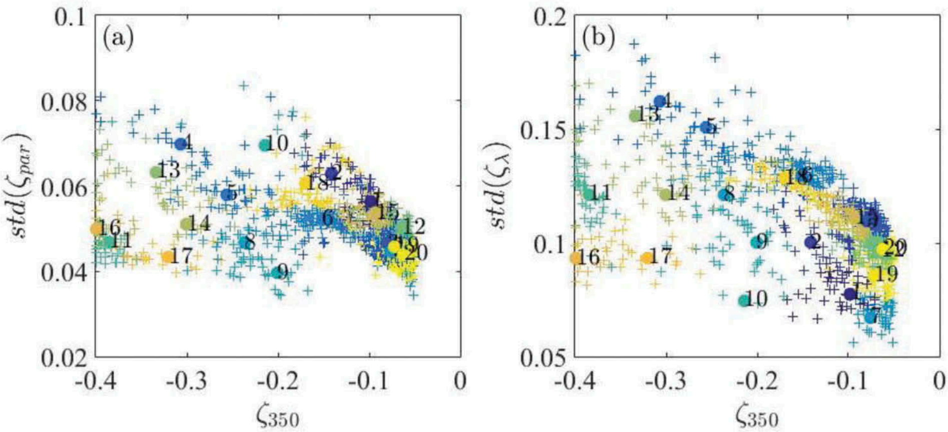

Figure 4. Robustness index of suspension parameters and equivalent conicity.

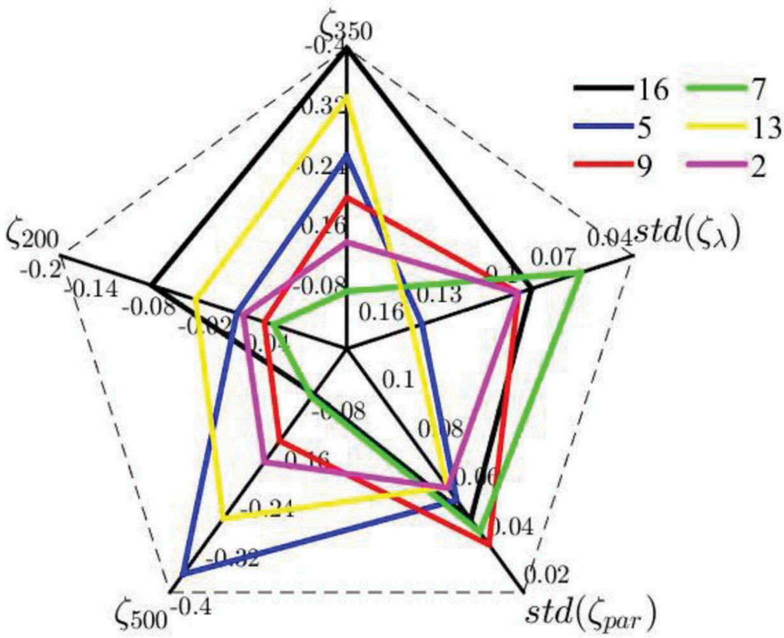

Figure 5. Objective values of the six cluster centres.

$std(\zeta_{par})$, and $std(\zeta_{\zeta})$ corresponding to 5th, 9th, and 7th clusters are the smallest, respectively. The 13th and 2nd clusters are typical parameter sets that take into account the trade-off of the five objectives, with which the system performances are in balance. The suspension parameters corresponding to the six cluster centres are shown in Table 2. Based on the vehicle dynamics analysis in section 4, the suspension parameter matching type of 16th, 5th, 9th, and 13th clusters is defined as the Type 1, and the parameter matching type of 7th and 2nd clusters is defined as the Type 2.

Table 2. Suspension parameters of the six cluster centres.

Cluster	*kpx* (N/m)	*kpy* (N/m)	*csx* (N s/m)	*csy* (N s/m)	*kncsx* (N/m)	*kncsy* (N/m)	Matching type
16	4.07E+07	5.94E+06	4.61E+06	3.41E+04	1.17E+07	2.67E+07	1
5	2.44E+07	1.41E+07	2.99E+06	3.07E+04	3.15E+07	1.94E+07	1
9	1.79E+07	7.51E+06	4.70E+06	1.71E+04	2.44E+07	1.49E+07	1
7	4.40E+07	2.57E+07	7.21E+05	2.52E+04	3.36E+07	1.41E+07	2
13	2.50E+07	7.43E+06	3.00E+06	3.62E+04	2.35E+07	1.16E+07	1
2	1.07E+08	4.40E+06	8.30E+05	3.62E+04	1.81E+07	2.11E+07	2

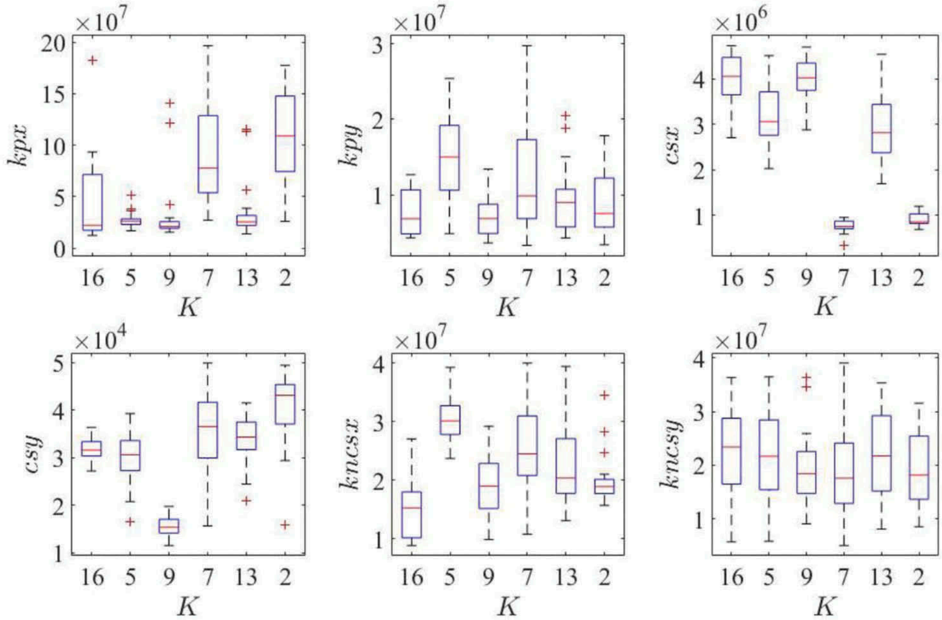

Figure 6. Suspension parameter distribution of the six clusters.

Figure 6 reflects the distribution of corresponding six groups suspension parameters of the selected six clusters, and it is represented by a Box-plot. The number of parameter sets corresponding the six clusters is 19, 37, 28, 54, 25, and 32, respectively. The emphasized optimization objective of each cluster is different, and the matching rules of suspension parameters for the corresponding objectives can be obtained by observing the graphs. It can be seen from the graph that *kpy* and *kncsy* have no obvious influence on the system stability, which can also be confirmed from the correlation analysis in section 4. For the suspension parameters of 16th cluster, the stability indexes ζ_{200} and ζ_{350} are better, and a smaller *kncsx* and a larger *csx* are beneficial to the two indexes. For the 5th cluster, the stability index ζ_{500} is better, where a smaller *kpx* as well as a larger *csx* and *kncsx* are beneficial to the system hunting stability under the ultra-high speed condition. For the 9th cluster, the suspension parameters robustness index $std(\zeta_{par})$ is the best, and a smaller *kpx*, *csy* as well as a larger *csx* are beneficial to the index. For the 7th cluster, the equivalent conicity robustness index $std(\zeta_{\zeta})$ is the best, and a larger *kpx* as well as a smaller *csx* improves the equivalent conicity robustness.

According to the analysis of the suspension parameter distribution of the Pareto set, two types of suspension parameters matching rules for improving vehicle hunting stability robustness can be summarized. The first one is the matching of small primary longitudinal stiffness *kpx* with large yaw damping *csx*. The second one is the matching of large primary longitudinal stiffness *kpx* with small yaw damping *csx*. The 13th and 2nd clusters are selected to represent the two types of the typical matching rules, with which the multiple optimal indexes are taken into account, and the vehicle dynamic performances are more balanced. Compared with 2nd cluster, the stability margin of vehicle system adopting the suspension parameters of 13th cluster is larger, but the equivalent conicity robustness is worse, while the suspension parameters robustness are equal. The two types of suspension parameters matching rules are consistent with the two types of high-speed trains currently in service in China.

In order to analyse the system hunting stability of the vehicle corresponding to the six groups of suspension parameters in Table 2, the linear stability index of the vehicle with the variation of equivalent conicity and running speed is calculated as shown in Figure 7. It can be observed from the graphs that the change of the running speed has a little effect on the hunting stability when the variation range of the stability index along the longitudinal axis is small, which suggests that the system has strong speed robustness. The influence of the running speed on the stability of the vehicle with low equivalent conicity is smaller than the vehicle with high equivalent conicity. When the stability index changes little along the abscissa axis, the equivalent conicity robustness of the vehicle is better. It can be drawn from the figure that the stability of the vehicle adopting different suspension parameters has significantly different effects with the variation of equivalent conicity and running speed.

For the 16th, 5th, and 13th clusters, there are larger stability regions, and the stability of the 16th cluster is better at low equivalent conicity, while the 5th cluster is better at

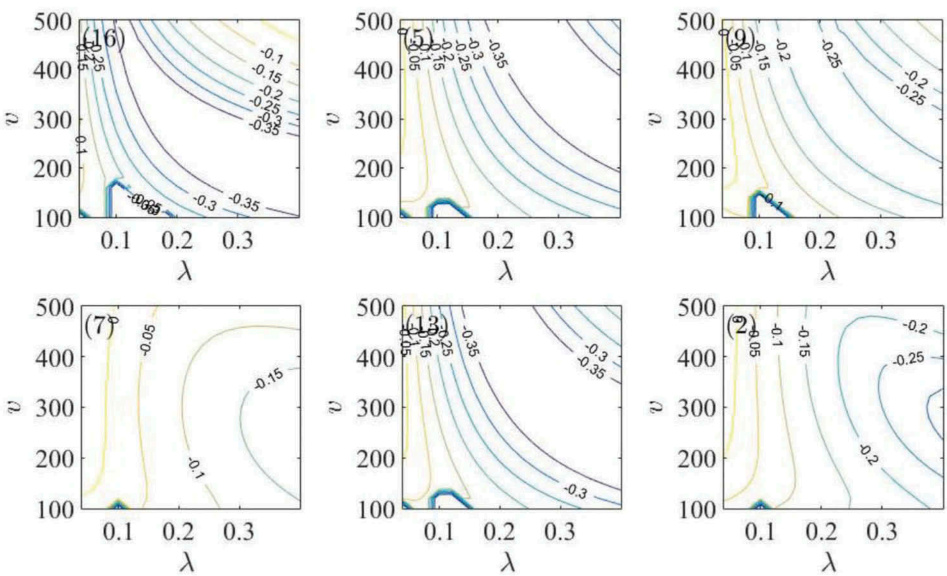

Figure 7. Vehicle stability index at different speed and equivalent conicity.

high speed. The stability regions of 7th and 2nd clusters are smaller, but the system stability is less affected by the variation of vehicle speed and equivalent conicity. When the vehicle adopts the suspension parameters of Type 2, a larger equivalent conicity tread is needed to ensure the vehicle hunting stability. No matter which type of suspension parameter is adopted, the system stability will become worse if the equivalent conicity of wheel-rail contact is too small. With the increase of running speed and equivalent conicity, the variation of vehicle system stability corresponding to the six groups of suspension parameters is inconsistent, so it can be inferred that the bifurcation forms of the vehicle non-linear stability will be different.

4. Optimal matching of suspension parameters

4.1. Speed robustness

The root loci of the vehicle system with the change of running speed according to the six groups of suspension parameters are shown in Figure 8. Each root locus is composed of 40 sets of characteristic roots in the speed range of 20–800 km/h, and each '+' indicates a corresponding mode. The larger symbol represents a larger running speed. The horizontal axis indicates the mode damping ratio ζ (negative sign indicates a stable value), which is the ratio of the real part to the modulus of eigenvalues of the system matrix. The vertical axis indicates the damped vibration frequency of mode, which is the imaginary part of eigenvalues. Normally, as the speed increases, the hunting-related mode's damping reduces. When the ζ is greater than 0, the hunting movement is

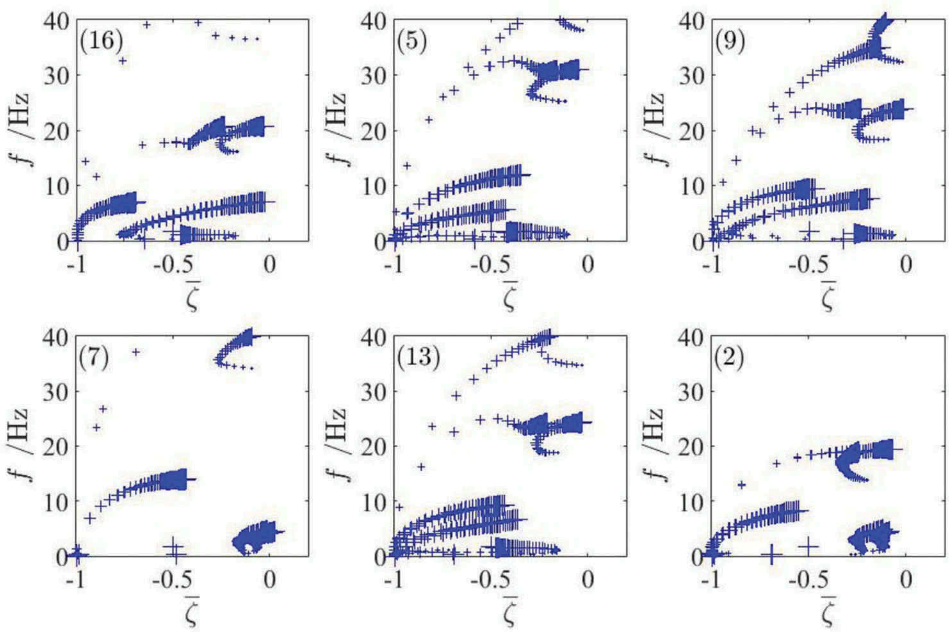

Figure 8. Root loci of the vehicle with the change of speed.

unstable. Mostly, the low-frequency hunting mode (1-5 Hz) determines the vehicle hunting critical speed.

Comparing the speed root locus of the vehicle system with the six groups of suspension parameters, it can be found that the root locus curve is consistent with the classification of the suspension parameter type. Type 1 adopts the rule that a smaller *kpx* matches a larger *csx*, and the stability of the bogie hunting mode with frequency below 2 Hz is enhanced with the increasing vehicle speed, such as the suspension parameters according to 16th, 5th, 9th, and 13th clusters. Type 2 adopts opposite rule that a larger *kpx* is matched with a smaller *csx*, with which the hunting mode with frequency range of 1 ~ 4 Hz affects the linear stability of the vehicle system. The stability of bogie hunting mode decreases with the increase of the vehicle speed, such as the suspension parameters according to 7th and 2nd clusters.

The stability of the vehicle adopting the suspension parameter corresponding to the 16th cluster is better at the speed of 200 km/h and 350 km/h, while the vehicle corresponding to 5th cluster has a better stability at ultrahigh speed, which has a good stable margin for speed. The vehicle adopting the suspension parameters based on 7th and 2nd clusters has poor a stability margin, but the variation on the system stability index is small with the change of running speed. This is consistent with the results in the radar chart of Figure 5.

Each suspension parameter is normally distributed within a certain range, and the suspension parameters are combined randomly with each other. Furthermore, the stability index of the vehicle with the random combined parameters is calculated, respectively. Therefore, the influence of the suspension parameters on the stability of the vehicle system can be evaluated by the suspension parameter robustness index. Take the 16th cluster suspension parameters as an example, Figure 9 shows the influence of suspension parameter distribution on the system stability of the vehicle at the speed of 350 km/h. The abscissa axis represents the scaling coefficient of suspension parameters, and the vertical axis represents the vehicle stability index ζ_{350}. It can be drawn from the figure that the system stability index decreases with the increasing *csy*, and the corresponding vehicle hunting stability improves. Namely, ζ_{350} is negatively correlated with *csy* for this group of suspension parameter.

In order to analyse the correlation between the index and each suspension parameter, the regression coefficient was calculated utilizing the method of partial least-squares regression [27]. Partial least-squares regression coefficient β (hereinafter called regression coefficient) between ζ_{350} calculated under the 6 groups of suspension parameters and each suspension parameter is shown in Figure 10. The higher the histogram in the figure, the stronger the correlation among the corresponding parameter and system performance indexes is. If the correlation between the suspension parameter and the system performance index is weak, it indicates that the group of suspension parameters is reasonable for the performance index. The calculated regression coefficient $\beta[\zeta_{200}]$ and $\beta[\zeta_{500}]$ at the speed of 200 and 500 km/h are shown in Tables 3 and 4, respectively. Based on the correlation analysis of the ζ_{200}, increasing *csy* and decreaseing *kncsx* lead to the reduction of the index value of ζ_{200}, improving the hunting stability of the vehicle system at speed of the 200 km/h. According to the ζ_{350}, increasing *csy* as well as decreasing *kpx, csx,* and *kncsx* result in the diminution of ζ_{350} for the suspension parameters of Type 1. For the suspension parameters of Type 2, such as 7th and 2nd

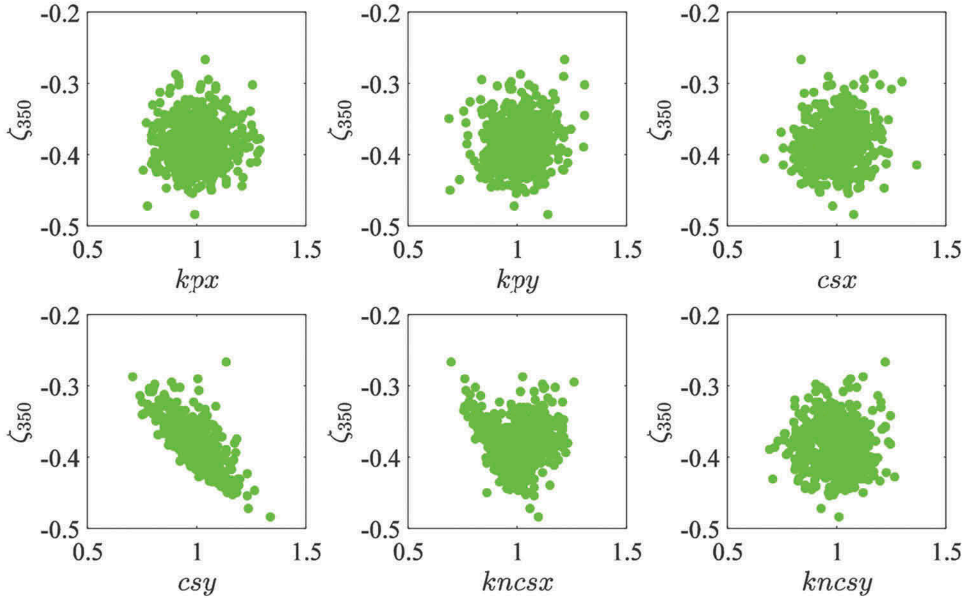

Figure 9. The ζ_{350} with scaling of suspension parameters of 16th cluster.

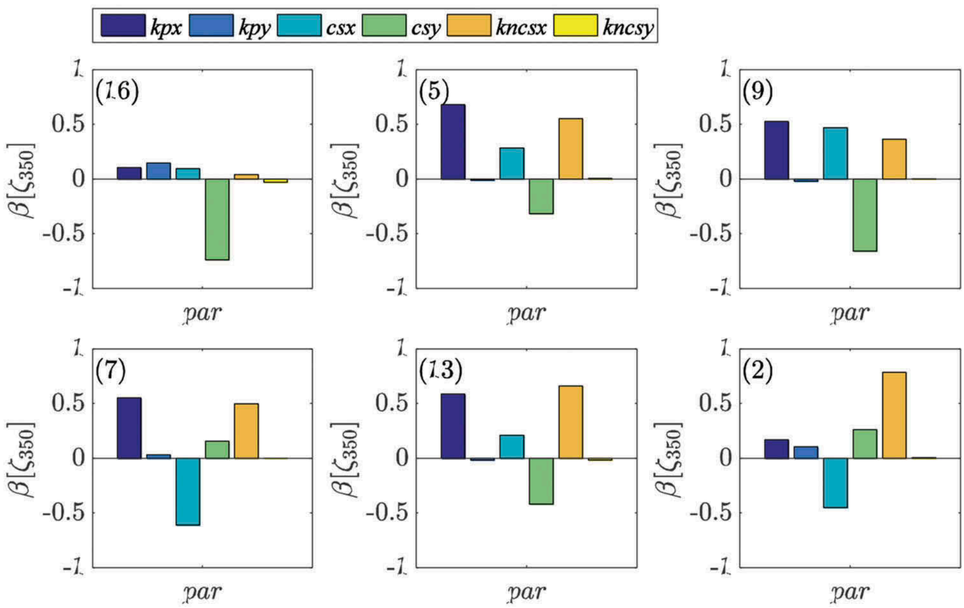

Figure 10. Correlation analysis between ζ_{350} and suspension parameters.

clusters, increasing *csx* is conducive to reducing ζ_{350}. Corresponding to the ζ_{500}, increasing *kncsx* is beneficial to reducing ζ_{500} for the suspension parameters of Type 1. For the suspension parameter of Type 2, increasing *csx* is conducive to reducing ζ_{500}, and improving the vehicle hunting stability at the speed of 500 km/h.

Table 3. Correlation analysis between ζ_{200} and suspension parameters.

	β [ζ_{200}]					
Cluster	*kpx*	*kpy*	*csx*	*csy*	*kncsx*	*kncsy*
16	0.04	−0.05	−0.69	0.66	−0.00	0.04
5	0.02	0.01	−0.70	0.37	0.01	0.02
9	0.01	0.11	−0.69	0.33	0.00	0.01
7	0.09	0.36	−0.14	0.44	0.00	0.09
13	0.01	−0.07	−0.67	0.51	−0.00	0.01
2	0.40	0.12	−0.23	0.84	−0.02	0.40

Table 4. Correlation analysis between ζ_{500} and suspension parameters.

	β [ζ_{500}]					
Cluster	*kpx*	*kpy*	*csx*	*csy*	*kncsx*	*kncsy*
16	−0.11	0.37	−0.00	−0.27	−0.90	−0.00
5	−0.47	0.00	0.02	−0.23	−0.77	−0.01
9	−0.59	0.09	0.01	−0.15	−0.81	−0.00
7	0.38	0.02	−0.87	−0.06	0.27	−0.00
13	−0.40	0.14	0.02	−0.27	−0.88	0.00
2	0.11	0.24	−0.88	−0.21	0.18	0.02

4.2. Suspension parameter robustness

Each suspension parameter is normally distributed within a certain range and the suspension parameters are combined randomly with each other. Furthermore, the standard deviation of system stability index is calculated, which defined as the vehicle suspension parameter robustness index. According to this method, the sensitivity of vehicle suspension parameters on the hunting stability can be evaluated. Take the 16th cluster as an example, the calculation results of this group of suspension parameters are shown in Figure 11. The abscissa axis represents the scaling coefficient of suspension parameters, and the vertical axis represents the suspension parameter robustness index $std(\zeta_{par})$. Figure 12 shows the regression coefficient β between suspension parameters robustness indexes calculated under the 6 groups of suspension parameters and each suspension parameter. There are remarkable distinctions in the influence law between the each group of parameters. The smaller the height of the histogram implies that the influence of the suspension parameter on $std(\zeta_{par})$ is smaller. For the suspension parameters of Type 1, increasing *csx* as well as decreasing *csy* and *kncsx* is beneficial to improve the vehicle suspension parameters robustness. For the suspension parameters of Type 2, increasing *kpx, kncsx* and decreasing *csx* are beneficial to enhance the vehicle suspension parameters robustness.

4.3. Equivalent conicity robustness

The root loci of the vehicle system with the change of equivalent conicity according to the six groups of suspension parameters are shown in Figure 13, in which the vehicle running speed is 350 km/h. Each root locus curve is composed of 25 sets of characteristic roots in the equivalent conicity range of 0.02–0.5, and each 'o' indicates a corresponding mode. The larger symbol represents a larger equivalent conicity. The horizontal axis indicates the mode damping ratio ζ (negative sign indicates a stable value), which is the ratio of the real part to the modulus of eigenvalues of the system matrix. The vertical axis indicates the damped vibration frequency

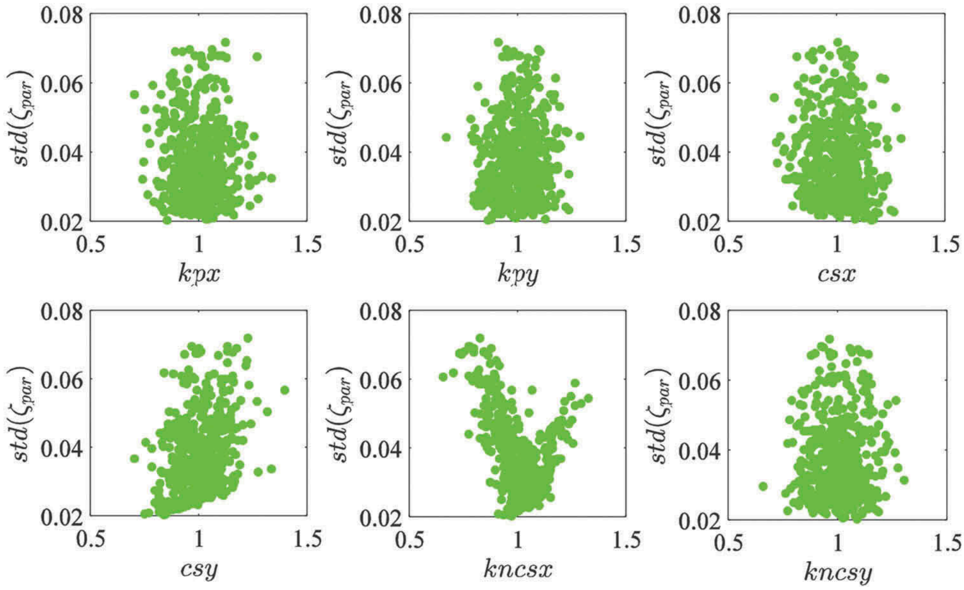

Figure 11. The $std(\zeta_{par})$ with scaling of suspension parameters of 16th cluster.

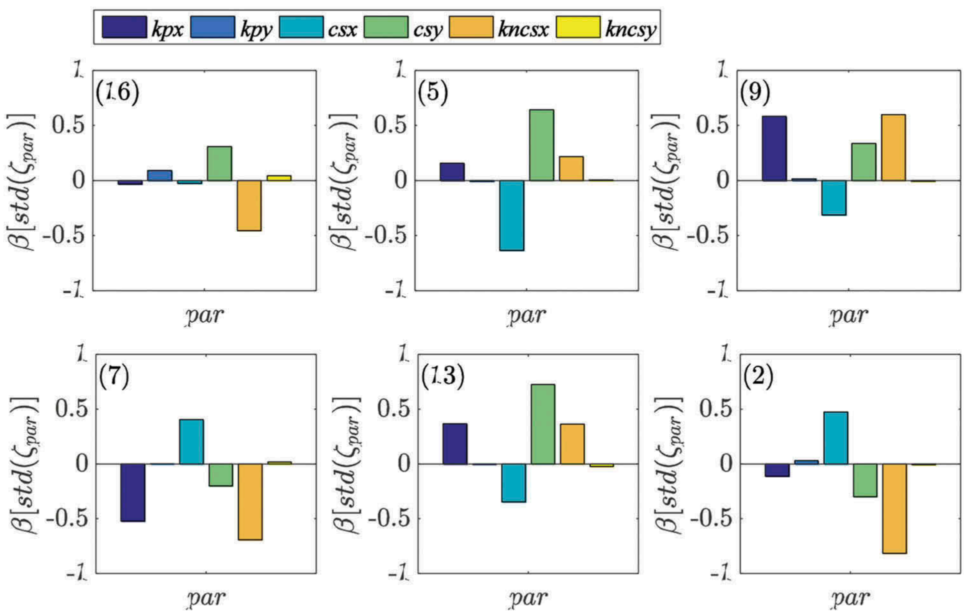

Figure 12. Correlation analysis between $std(\zeta_{par})$ and suspension parameters.

of the mode, which is the imaginary part of eigenvalues. When the ζ is greater than 0, the hunting movement is unstable. Mostly, the low-frequency hunting mode (1-5 Hz) determines the vehicle hunting critical speed. Normally, as the equivalent conicity increases, the hunting-related mode damping increases first and then decreases.

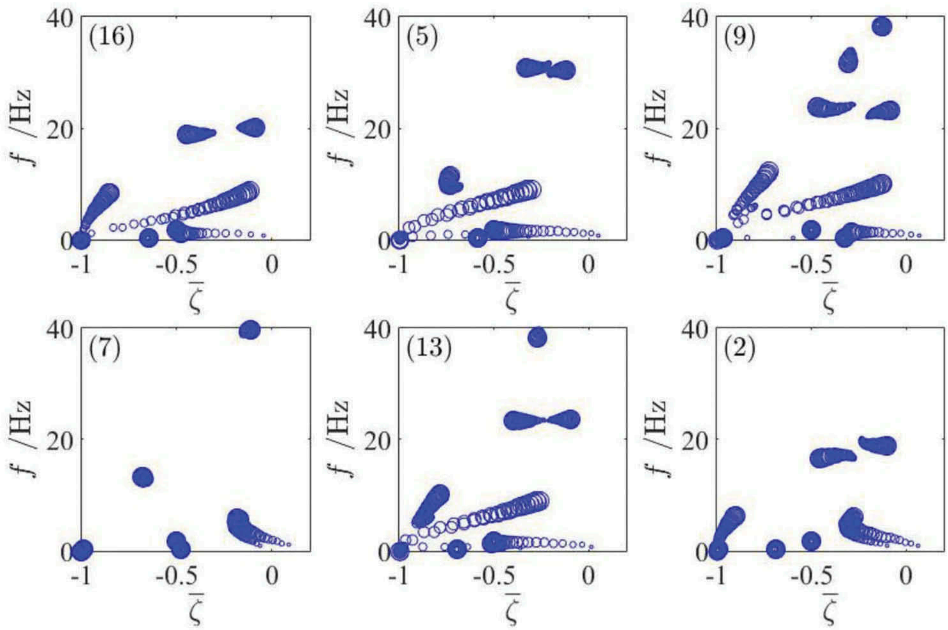

Figure 13. Root loci of the vehicle with the change of equivalent conicity.

In the figure, when the normal equivalent conicity of the vehicle is located at the turning position of the bogie hunting root locus, the equivalent conicity robustness index of the vehicle is small. The small vehicle equivalent conicity robustness index indicates that the hunting stability is insensitive to the variation of the wheel-rail contact equivalent conicity. In other words, the vehicle has strong adaptability to the track variation, such as variable rail cant and rail head profile, as well as a long repair period for the tread, which reduces the costs of vehicles operation and maintenance. It is observed from the figure that the stability of the vehicle corresponding to the suspension parameters of 7th and 2nd clusters is less affected by the variation of the equivalent conicity. In fact, the vehicle hunting instability due to the low wheel-rail contact equivalent conicity occurs occasionally, especially in the situation of a new tread profile or larger rail cant. By means of increasing the hunting stability of the vehicle, the equivalent conicity robustness and the system stability with low equivalent conicity of the vehicle are better, such as the suspension parameters of the 16th cluster. But the excessive stability margin will reduce the lateral displacement of the wheel-rail contact point, resulting in the local tread wear easily.

Similarly, the influence of the suspension parameter matching on the equivalent conicity stability can be evaluated according to the method of random parameters. The regression coefficient β among $std(\zeta_\zeta)$ and each suspension parameter is shown in Figure 14. For suspension parameters of Type 1, decreasing *kncsx* and increasing *csx* are beneficial to improve the vehicle equivalent conicity robustness. For the suspension parameters of Type 2, decreasing *csx* and increasing *kncsx* are beneficial to the vehicle equivalent conicity robustness.

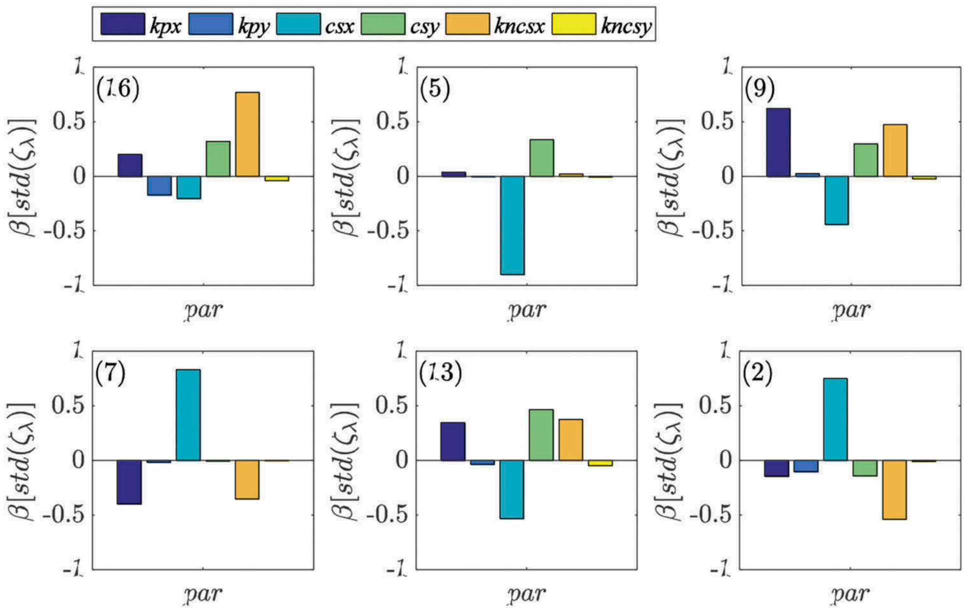

Figure 14. Correlation analysis between $std(\zeta_\zeta)$ and suspension parameters.

5. Conclusion

(1) The concept of robust hunting stabilities is proposed, and the running speed robustness, suspension parameter robustness, and equivalent conicity robustness for vehicle system are defined. Based on the robustness indexes, the key suspension parameters of bogie affecting the vehicle hunting stability are optimized. The genetic algorithm of NSGA-II is adopted to calculate the Pareto frontier of multiple objectives and Pareto set of vehicle optimal suspension parameters. The vehicle system has better robustness indexes by adopting the optimized suspension parameters to improve the adaptability for the variation of suspension parameters, tread profile, as well as track, such as variable rail cant and rail head profile, in a wide speed range.

(2) Six groups of typical suspension parameters are obtained by cluster analysis for the optimization results, and the corresponding robustness indexes for the vehicle hunting stability are analysed. Two typical optimization and matching rules of key suspension parameters of bogies for high-speed trains based on hunting stability robustness are obtained. The first one is the matching of small primary longitudinal stiffness with large yaw damping, with which the hunting stability and suspension parameters robustness of the vehicle system are better. The second one is the matching of large primary longitudinal stiffness with small yaw damping, with which the vehicle speed robustness and equivalent conicity robustness are better, but the tread with a larger equivalent conicity is required to ensure the vehicle hunting stability.

(3) The correlations among suspension parameters and each index are analysed by multivariate statistical analysis, which indicates the optimization direction for the

suspension parameters. When the correlation among suspension parameters and the optimized index is small, it indicates that the optimization and matching for suspension parameters are better. For the suspension parameters of Type 1, reducing the *csx* and *kncsx*, as well as increasing the *csx* is conducive to improving the vehicle system stability, the suspension parameter robustness as well as the equivalent conicity robustness. For the suspension parameters of Type 2, increasing the *kpx* and *kncsx*, as well as reducing *csx* is beneficial to vehicle system stability and suspension parameter robustness. Besides, the *csx* has strong correlation with the equivalent conicity robustness index, and reducing *csx* is conducive to improving the vehicle equivalent conicity robustness.

Disclosure statement

No potential conflict of interest was reported by the authors.

Funding

The material in this paper is based on work supported by grants (51675443, 51735012) from the National Natural Science Foundation of China, Sichuan Science and Technology Program grant (2018JY0209), and Traction Power State Key Laboratory grant (No.2018TPL_T05, No.2017TPL_T02) of the Independent Research and Development Projects;Traction Power State Key Laboratory grant [2017TPL_T02,2018TPL_T05].

References

[1] Yao Y, Li G, Sardahi Y, et al. Stability enhancement of a high-speed train bogie using active mass inertial actuators. Veh Syst Dyn. 2019;57(3):389–407.
[2] Yao Y, Wu G, Sardahi Y, et al. Hunting stability analysis of high-speed train bogie under the frame lateral vibration active control. Veh Syst Dyn. 2018;56(2):297–318.
[3] Zhang XX, Wu GS, Li G, et al. Actuator optimal placement studies of high-speed power bogie for active hunting stability. Veh Syst Dyn. 2019;57. DOI:10.1080/00423114.2019.1566556.
[4] Goodall RM. KortümW.Mechatronic developments for railway vehicles of the future. Control Eng Pract. 2002;10(8):887–898.
[5] Pearson JT, Goodall RM, Mei TX, et al. Active stability control strategies for a high speed bogie. Control Eng Pract. 2004;12(11):1381–1391.
[6] Mei TX, Goodall RM. Stability control of railway bogies using absolute stiffness: sky-hook spring approach. Veh Syst Dyn. 2006;44:83–92.
[7] Jiang JZ, Matamoros-Sanchez AZ, Goodall RM, et al. Passive suspensions incorporating inerters for railway vehicles. Veh Syst Dyn. 2012;50:263–276.
[8] Bruni S, Goodall R, Mei TX, et al. Control and monitoring for railway vehicle dynamics. Veh Syst Dyn. 2007;45(7–8):743–779.
[9] Li X, Ren ZS, Xu N. Dynamic performance analysis of high-speed vehicle based on optimization of bogie suspension parameters and tread conicity. J China Railway Soc. 2018;40(3):39–44.
[10] He Y, McPhee J. Design optimization of rail vehicles with passive and active suspensions: A combined approach using genetic algorithms and multibody dynamics. Veh Syst Dyn. 2002;37(Suppl.):397–408.
[11] He Y, McPhee J. Optimization of the lateral stability of rail vehicles. Veh Syst Dyn. 2002;38 (5):361–390.

[12] Yao Y, Zhang -X-X, Zhang H-J, et al. The stability mechanism and its application to heavy haul couplers with arc surface contact. Veh Syst Dyn. 2013;51(9):1324–1341.
[13] Karin NC, Berggren EG, Kaynia AM, et al. A new method for estimation of critical speed for railway tracks on soft ground. Int J Rail Transp. 2018;6(4):203–217.
[14] Wu SC, Xu ZW, Liu YX, et al. On the residual life assessment of high-speed railway axles due to induction hardening. Int J Rail Transp. 2018;6(4):218–232.
[15] Kodiyalam S, Sobieski J. Multidisciplinary design optimization—some formal methods, framework requirements, and application to vehicle design. Int J Vehicle Des. 2001;25(1/2):3–22.
[16] Mohebbi M, Rezvani MA. Multi objective optimization of aerodynamic design of high speed railway windbreaks using lattice boltzmann method and wind tunnel test results. Int J Rail Transp. 2018;6(3):183–201.
[17] He Y, Mcphee J. Multidisciplinary optimization of multibody systems with application to the design of rail vehicles. Multibody Syst Dyn. 2005;14(2):111–135.
[18] Johnsson A, Berbyuk V, Enelund M. Pareto optimisation of railway bogie suspension damping to enhance safety and comfort. Veh Syst Dyn. 2012;50(9):1379–1407.
[19] Bideleh SM, Berbyuk V, Persson R. Wear/comfort Pareto optimisation of bogie suspension. Veh Syst Dyn. 2016;54(8):1053–1076.
[20] Bideleh SM. Robustness analysis of bogie suspension components Pareto optimised values. Veh Syst Dyn. 2017;55(8):1189–1205.
[21] Alonso A. Yaw damper modelling and its influence on the railway dynamic stability[J]. Veh Syst Dyn. 2011;49(8):1367–1387.
[22] Zhai W, Liu P, Lin J, et al. Experimental investigation on vibration behaviour of a CRH train at speed of 350 km/h. Int J Rail Transp. 2015;3(1):1–16.
[23] Götz G, Polach O. Verification and validation of simulations in a rail vehicle certification context. Int J Rail Transp. 2018;6(2):83–100.
[24] Yao Y, Yan YP, Hu ZK, et al. The motor active flexible suspension and its dynamic effect on the high-speed train bogie. J Dyn Sys Meas Control. 2017;140:064501.
[25] Yao Y, Zhang XX, Liu X. The active control of the lateral movement of a motor suspended under a high-speed locomotive. J Rail Rapid Transit. 2016;230(6):1509–1520.
[26] Deb K, Agrawal RB. Simulated binary crossover for continuous search space. Complex Syst. 1995;9(2):115–148.
[27] Anderson TW. An introduction to multivariate statistical analysis. 3rd ed. Hoboken (US): John Wiley & Sons; 2003.

Appendix

Table A1. The vehicle model parameters.

Symbol	Definition	Value
m_w	Mass of the wheelset	1639 kg
I_w	Yaw inertia of the wheelset	822 kg m^2
m_f	Mass of bogie frame	2328 kg
I_{fx}	Roll inertia of bogie frame	2110 kg m^2
I_{fz}	Yaw inertia of bogie frame	4080 kg m^2
m_c	Mass of carbody	38,936 kg
I_{cx}	Roll inertia of carbody	1.67e6 kg m^2
I_{cy}	Yaw inertia of carbody	9.61e5 kg m^2
k_{pz}	Primary vertical stiffness per axle	0.75 kN/mm
k_{sx}	Secondary longitudinal stiffness	0.133 kN/mm
k_{sy}	Secondary lateral stiffness	0.133 kN/mm
k_{sz}	Secondary vertical stiffness	0.2 kN/mm
c_{sz}	Secondary vertical damper damping	10 kN s/m
c_{pz}	Primary vertical damper damping	10 kN s/m
$k_{\varnothing}$	Stiffness of anti-roll torsion bar	4.15 MN m/rad
$2l_1$	Lateral spacing of primary suspension	2000 mm
l_b	Length of axle box arm	480 mm
$2b$	Wheel base	2500 mm
$2L$	Length between bogie centers	17,375 mm
$2l_0$	Distance of the contact spot	1493 mm
$2l_2$	Lateral spacing of the secondary suspension	2200 mm
r_0	The wheel rolling radius	460 mm
$f\zeta$	The longitudinal creep coefficient	1e7 N
f_n	The lateral creep coefficient	1e7 N
k_r	The contact stiffness of the wheel–rail	500 kN/mm
ζ_e	Wheel–rail contact conicity	0.05, 0.17, 0.30
v	Running speed	200, 350, 500 km/h
k_{px}	Primary longitudinal stiffness per axle	*Optimized*
k_{py}	Primary lateral stiffness per axle	*Optimized*
c_{sx}	Yaw damper damping	*Optimized*
c_{sy}	Secondary lateral damper damping	*Optimized*
k_{nx}	Series stiffness of yaw damper damping	*Optimized*
k_{ny}	Series stiffness of secondary lateral damper damping	*Optimized*